

# A Simple Parcel Theory Model of Downdrafts in Atmospheric Convection

Thomas D. Schanzer



Taste of Research 2021

Supervisor: Prof. Steven Sherwood

School of Physics  
Faculty of Science  
University of New South Wales  
Sydney, Australia

## Abstract

Abstract

## Acknowledgements

The author is most grateful to his supervisor, Prof. Steven Sherwood, for his patient guidance and mentorship during the ten-week research project whose outcomes are documented in this report. The author also thanks the members of Prof. Sherwood's research group at the UNSW Climate Change Research Centre for some useful suggestions and feedback.

The author would also like to thank the UNSW School of Physics for offering the Taste of Research program under which this project was conducted, and in particular the program coordinator, A. Prof. Sarah Martell. The program has proved to be a very valuable and enjoyable learning opportunity.

## Data availability statement

All Python scripts and notebooks used to produce the results in this report are publicly available at <https://github.com/tschanzer/taste-of-research-21T3>.

## Notation for thermodynamic variables and constants

$p$	Total pressure
$z$	Height
$T$	Absolute temperature
$T_W$	Wet bulb temperature
$\rho$	Density
$q$	Specific humidity
$q^*(p, T)$	Saturation specific humidity
RH	Relative humidity
$\theta_e(p, T, q)$	Equivalent potential temperature
$l$	Ratio of liquid water mass to total
$L_v$	Latent heat of vapourisation of water
$c_p$	Specific heat at constant pressure of dry air
$R$	Specific gas constant of dry air
$g$	Acceleration due to gravity
$(\cdot)_E$	Environmental quantity
$(\cdot)_P$	Parcel quantity

# Contents

<b>1</b>	<b>Introduction and theory</b>	<b>4</b>
<b>2</b>	<b>Literature review</b>	<b>5</b>
2.1	Downdraft dynamics . . . . .	5
2.2	Thermodynamic calculations . . . . .	6
<b>3</b>	<b>Methods</b>	<b>6</b>
3.1	General approach and code structure . . . . .	6
3.2	Temperature as a function of pressure along a reversible moist adiabat . .	6
3.3	Temperature of an entraining, descending parcel . . . . .	6
3.4	Density, buoyancy and motion of a descending parcel . . . . .	10
<b>4</b>	<b>Results</b>	<b>11</b>
4.1	Downdraft initiation and initial conditions . . . . .	11
4.2	The impact of entrainment . . . . .	13
4.3	The impact of environmental humidity . . . . .	14
<b>5</b>	<b>Conclusions</b>	<b>17</b>

# 1 Introduction and theory

Along with updrafts, downdrafts—downward-moving masses of air—are important features in the dynamics of the Earth’s atmosphere; they transport mass, momentum, heat and moisture vertically and also generate and maintain storms (Knupp and Cotton 1985).

Indeed, one of the main objectives of present-day research into downdraft dynamics is to improve the predictions of global climate models (Thayer-Calder 2013), whose output informs the understanding of the larger-scale dynamics, including the pressing issue of anthropogenic climate change. Specifically, the high computational cost of running a global climate model over the necessarily large spatial domain and prediction timescales constrains their maximum resolution, which is still too coarse to describe convection. The models therefore employ schemes known as *parametrisations* which estimate the effect of convection on the state of the model using the information available at each time step; an accurate estimation requires a strong understanding of the factors that govern convection.

On a smaller scale, strong downdrafts that reach the Earth’s surface (*downbursts*) are known to cause significant damage to man-made structures and create hazardous, or even deadly, conditions for aircraft (Thayer-Calder 2013). Another aim of downdraft research is therefore to understand the mechanisms that generate such extreme events and improve the ability to predict them in advance.

Considering these motivations, the goal of this work is to gain insight into which processes and conditions initiate, and which maintain or inhibit, downdrafts. The approach will be to construct a significantly simplified model of a downdraft using *parcel theory*.

An air parcel is a mass of air with an imaginary flexible (but usually closed) boundary; under the usual assumptions, its exact size and shape are irrelevant. The only force assumed to act on the parcel is the net buoyant force (per unit mass), given in accordance with Archimedes’ principle by

$$b = \frac{\rho_E - \rho_P}{\rho_P} g. \quad (1)$$

If the parcel is lowered in the atmosphere to a location with a higher pressure, the work done to compress it and any heat exchanged will manifest as a change in its internal energy in accordance with the first law of thermodynamics. The second key assumption of parcel theory is that this process is adiabatic; this is valid due to the low thermal conductivity of air.

The potential presence of water in gas, liquid and solid phases in the parcel is a major complication; under the assumption that the parcel remains in phase equilibrium (i.e., changes are slow enough for excess liquid to evaporate if the vapour pressure is below the saturation value), there are two modes of adiabatic descent the parcel may undergo. If no liquid is present, the descent is *dry adiabatic* and the rate of work on the parcel causes it to warm at an approximate rate of  $9.8 \text{ K km}^{-1}$ . If liquid is present, the descent is *moist adiabatic*: progressive warming of the parcel raises its saturation vapour pressure, allowing the liquid to progressively evaporate during descent, with the necessary transfer

of latent heat from the air to the water creating an opposing cooling effect.

If the pressure and temperature of the parcel are thus known at any point in its descent, its density may be calculated using the ideal gas law,

$$\rho = \frac{p}{RT_v}, \quad (2)$$

where  $T_v$  is the *virtual temperature* that contains a small correction to account for the different density of water vapour. If an mass  $l$  of liquid water, per unit total parcel mass, is also present, it is easily shown that (assuming the liquid occupies negligible volume) the corrected parcel density is

$$\rho = \frac{p}{RT_v(1-l)}. \quad (3)$$

Knowledge of the parcel and environmental densities enable calculation of the buoyant force per unit mass on the parcel using (1), and its resulting displacement and velocity may be obtained by (numerically) solving the ODE

$$\frac{d^2z}{dt^2} = b(z). \quad (4)$$

## 2 Literature review

Possible items for discussion:

- Knupp and Cotton (1985): the downdraft types and their typical characteristics
- Thayer-Calder (2013): last chapter on the Lagrangian view of downdrafts
- Market et al. (2017): correlation between DCAPE and DCIN and downdraft strength
- Sumrall (2020): DCAPE, DCIN and severe surface winds
- Davies-Jones (2008): pseudoadiabatic wet bulb temperature approximations
- Bolton (1980): equivalent potential temperature and saturation vapour pressure approximations
- Saunders (1957): reversible moist adiabatic temperature approximation

### 2.1 Downdraft dynamics

Knupp and Cotton (1985) identify four downdraft types, which informed the methods of this investigation: penetrative, cloud-edge, overshooting and precipitation-associated. The penetrative type arises when subsaturated environmental air is *entrained* (mixed) into

saturated cloudy air, allowing evaporation of the excess liquid that creates negative buoyancy. The cloud-edge type, they note, is less understood and may result from evaporative cooling at the edges of clouds. An overshooting downdraft may be generated when the inertia of an updraft causes it to rise beyond its level of neutral buoyancy and subsequently sink. The precipitation-associated downdraft is generated by the evaporation of precipitation into subsaturated air beneath a cloud, with the cooling creating negative buoyancy. The model presented in this work most closely describes the precipitation-associated and penetrative types.

## **2.2 Thermodynamic calculations**

# **3 Methods**

## **3.1 General approach and code structure**

Mention general capabilities of the code

## **3.2 Temperature as a function of pressure along a reversible moist adiabat**

## **3.3 Temperature of an entraining, descending parcel**

Mixing and phase equilibration

Dry and/or reversible moist adiabatic descent

Finding temperature as a function of height

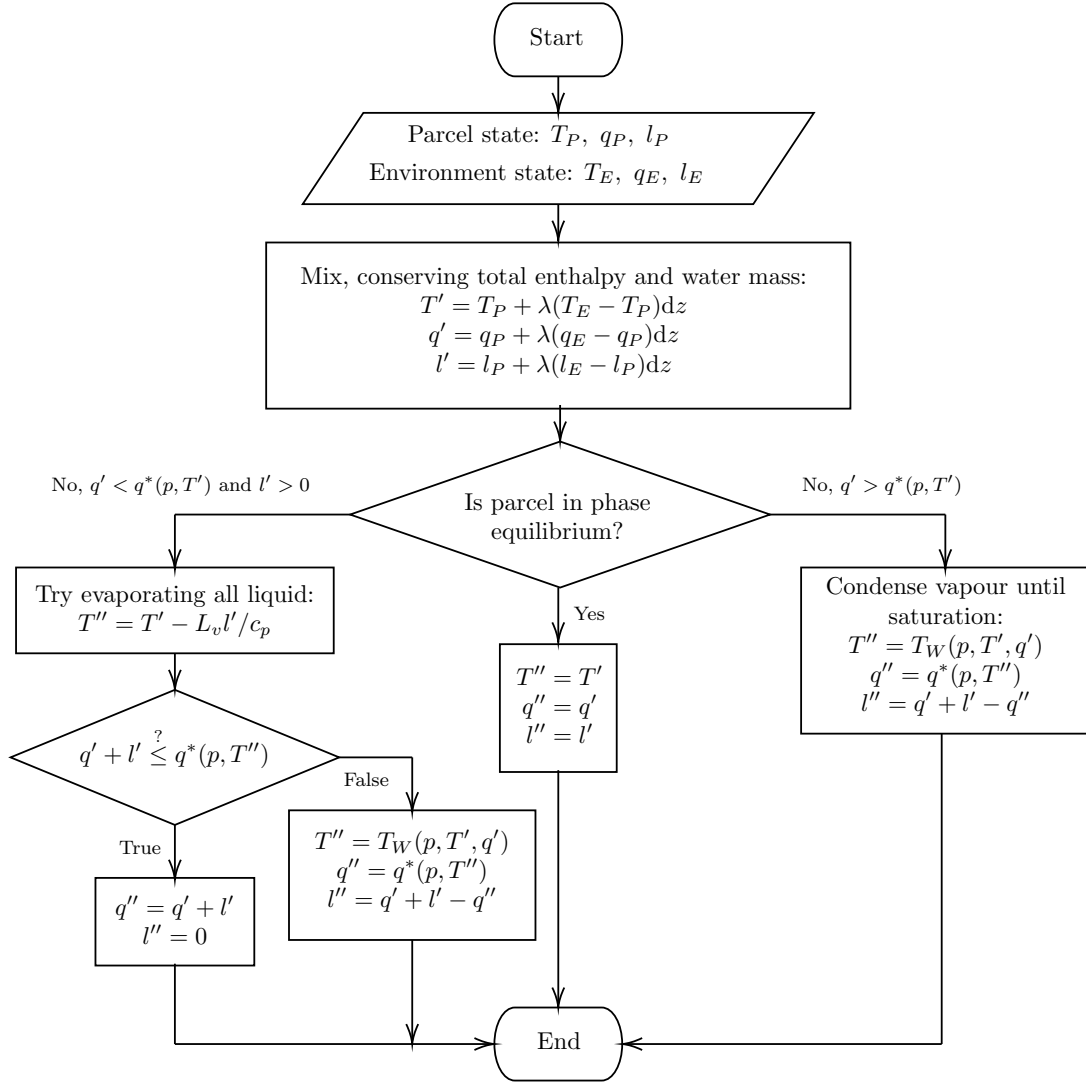


Figure 1: Flowchart for the mixing and phase equilibration calculation (functions `mix` and `equilibrate`) performed at each downward step for the entraining downdraft.

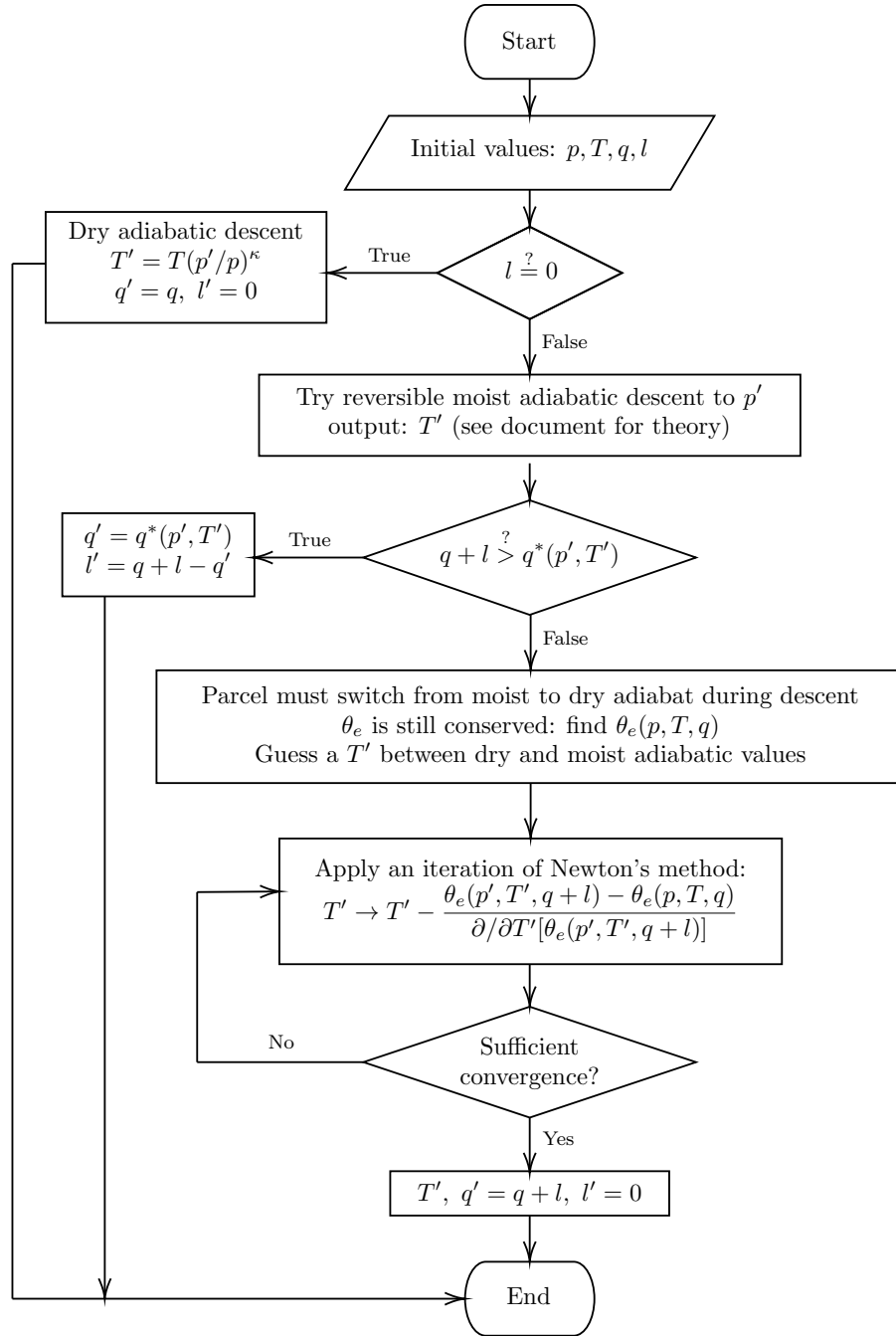


Figure 2: Flowchart for the descent calculation (**descend**) performed at each downward step for the entraining downdraft.



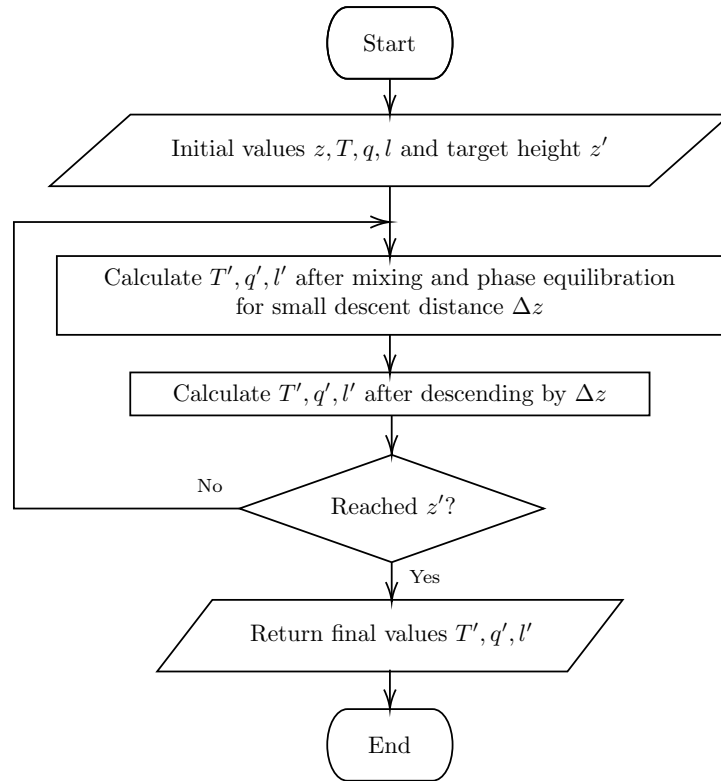


Figure 3: Flowchart for the calculation of parcel temperature as a function of height (`EntrainingParcel.profile`), assembling the routines shown in Figures 1 and 2.

### 3.4 Density, buoyancy and motion of a descending parcel

## 4 Results

### 4.1 Downdraft initiation and initial conditions

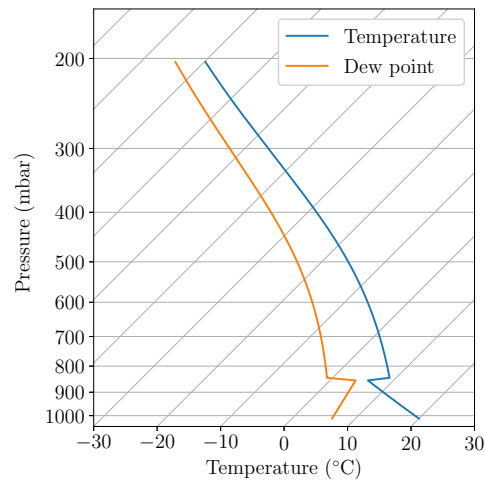


Figure 4: Skew  $T$ -log  $p$  plot of the idealised atmospheric sounding used in Section 4.1.

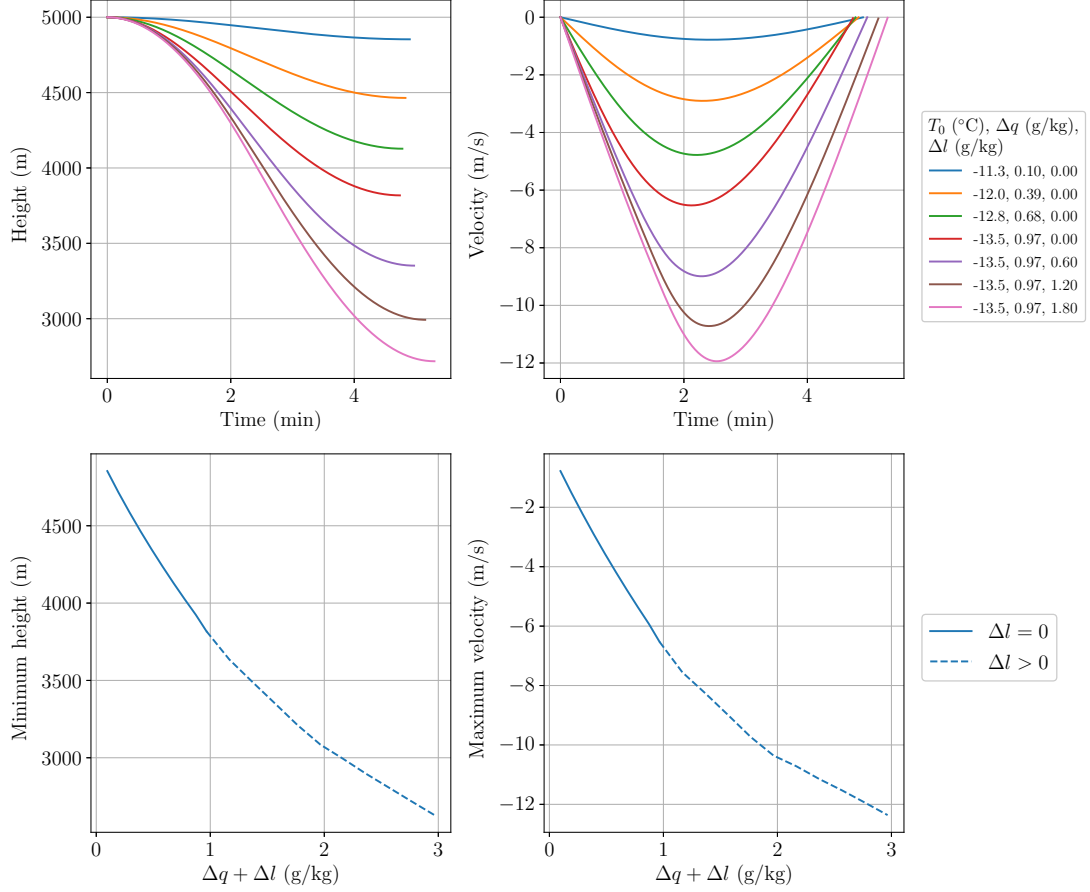


Figure 5: Properties of a downdraft parcel originating at height 5 km in an idealised atmospheric sounding with 50% relative humidity in the upper atmosphere and a fixed entrainment rate of  $1 \text{ km}^{-1}$ . Top row: height (left) and velocity (right) as functions of time, for selected initial conditions. Bottom row: minimum height reached (left) and maximum downward velocity (right) as functions of the total amount of water initially added to the parcel (specific humidity change due to evaporation  $\Delta q$  plus additional liquid water per unit parcel mass  $\Delta l$ ).

## 4.2 The impact of entrainment

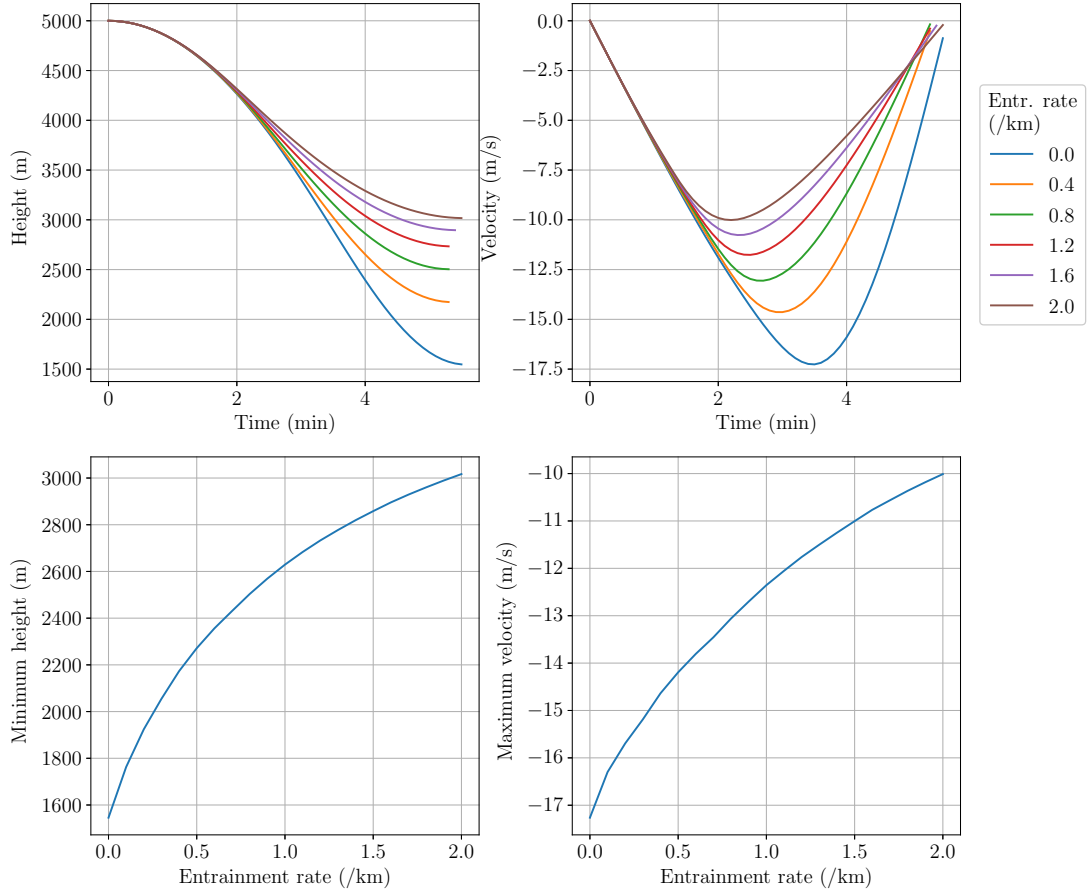


Figure 6: Properties of a downdraft parcel originating at height 5 km in an idealised atmospheric sounding with 50% relative humidity in the upper atmosphere. The initial conditions are fixed: an environmental parcel is brought to saturation by evaporation of liquid water, and  $2 \text{ g kg}^{-1}$  liquid water is additionally suspended in the parcel. Top row: height and velocity over time for selected entrainment rates. Bottom row: minimum height reached and maximum velocity as functions of entrainment rate.

### 4.3 The impact of environmental humidity

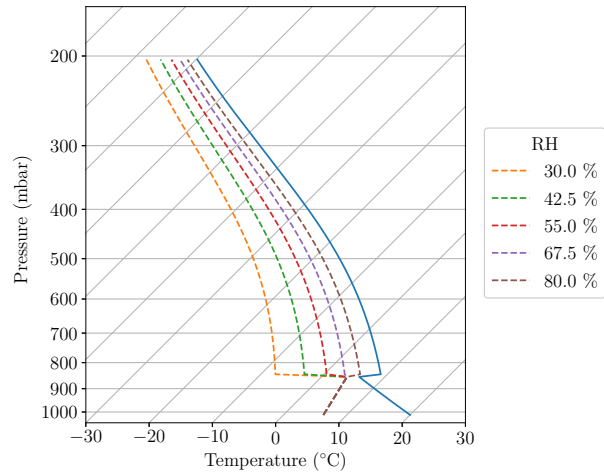


Figure 7: Skew  $T$ -log  $p$  plot of some selected idealised atmospheric soundings used in Section 4.3. The dashed lines on the left are the dewpoint profiles for the different soundings, and the solid blue line on the right is the common temperature profile.

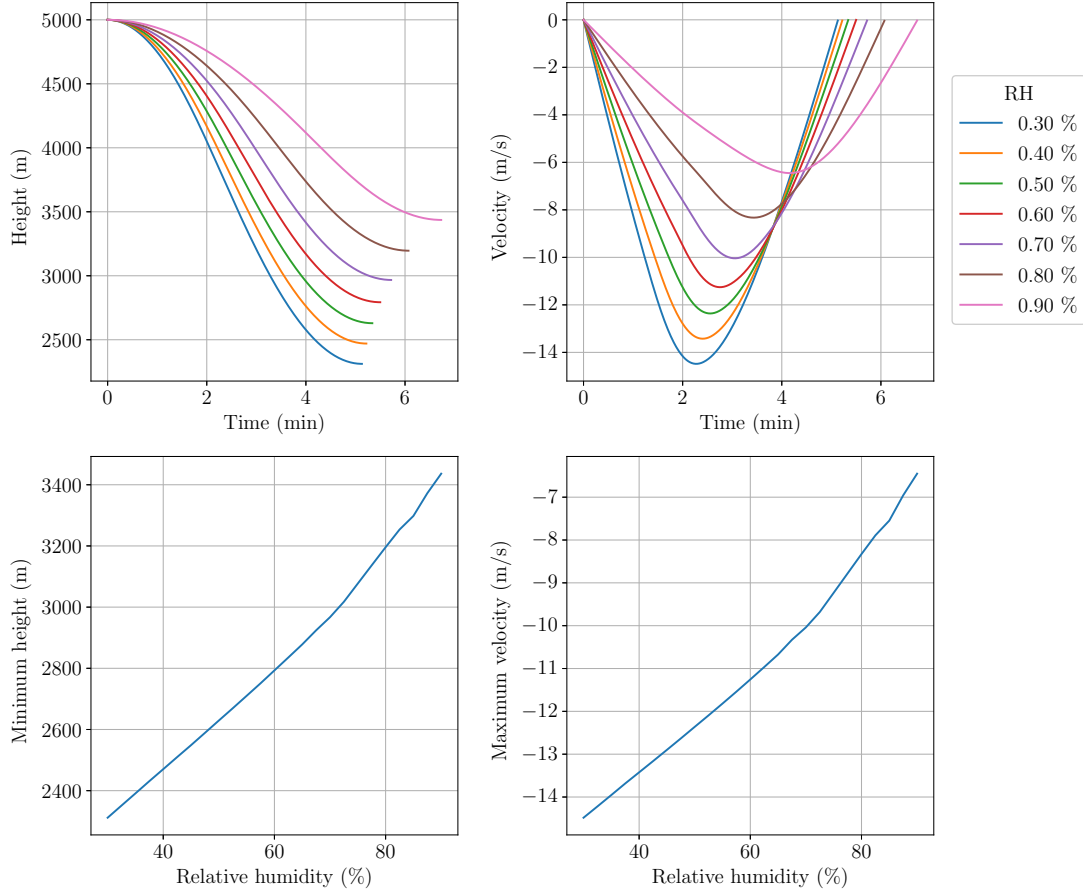


Figure 8: Properties of a downdraft parcel originating at height 5 km in idealised atmospheric soundings whose upper atmosphere relative humidities vary between 30% and 90%. The initial conditions are generated by bringing an environmental parcel to saturation by evaporation of liquid water (note that the resulting temperatures differ since more humid environmental parcels are closer to their wet bulb temperatures), and  $2 \text{ g kg}^{-1}$  liquid water is additionally suspended in the parcel. Top row: height and velocity of the parcel over time for selected soundings. Bottom row: minimum height reached and maximum downward velocity as functions of relative humidity in the upper atmosphere.

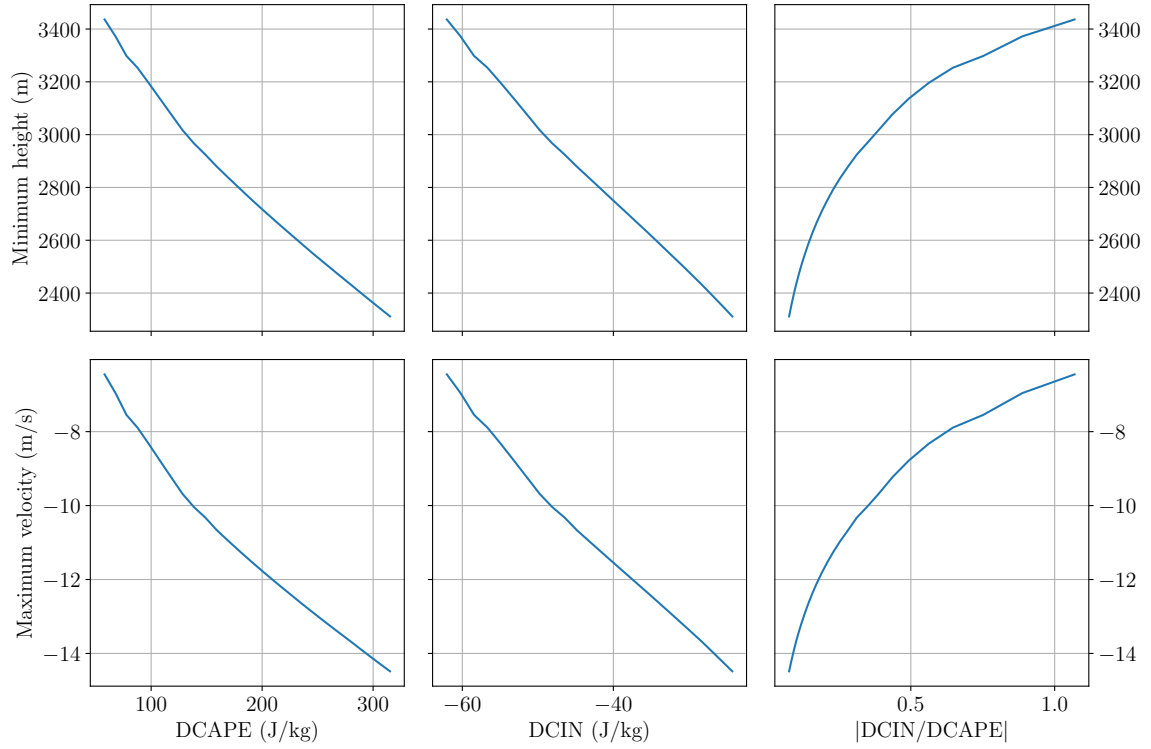


Figure 9: Plots of the minimum height (top row) and maximum downward velocity (bottom row) reached by the parcel of Figure 8 as functions of the downdraft convective available potential energy (DCAPE, left column), downdraft convective inhibition (DCIN, centre column) and the ratio  $|\text{DCIN}/\text{DCAPE}|$  (right column).



## 5 Conclusions

## References

- Bolton, David (1980). “The computation of equivalent potential temperature”. In: *Mon. Weather Rev.* 108.7, pp. 1046–1053. ISSN: 0027-0644.
- Davies-Jones, Robert (2008). “An efficient and accurate method for computing the wet-bulb temperature along pseudoadiabats”. In: *Mon. Weather Rev.* 136.7, pp. 2764–2785. ISSN: 0027-0644. DOI: 10.1175/2007MWR2224.1.
- Knupp, Kevin R and William R Cotton (1985). “Convective cloud downdraft structure: An interpretive survey”. In: *Rev. Geophys.* 23.2, pp. 183–215. ISSN: 8755-1209. DOI: 10.1029/RG023i002p00183.
- Market, P. S, S. M Rochette, J Shewchuk, R Difani, J. S Kastman, C. B Henson, and N. I Fox (2017). “Evaluating elevated convection with the downdraft convective inhibition”. In: *Atmos. Sci. Lett.* 18.2, pp. 76–81. ISSN: 1530-261X. DOI: 10.1002/asl.727.
- Saunders, P. M (1957). “The thermodynamics of saturated air: a contribution to the classical theory”. In: *Q. J. Roy. Meteor. Soc.* 83.357, pp. 342–350. ISSN: 0035-9009.
- Sumrall, Paula (2020). “Using DCIN and DCAPE to evaluate severe surface winds in the case of elevated convection”. masters thesis. University of Missouri.
- Thayer-Calder, Katherine (2013). “Downdraft impacts on tropical convection”. PhD thesis. Colorado State University.